

Screening effects in flow through rough channels

J. S. Andrade Jr.^{1,2,3}, A. D. Araújo¹, M. Filoche^{2,3}, and B. Sapoval^{2,3}

¹Departamento de Física, Universidade Federal do Ceará,
60451-970 Fortaleza, Ceará, Brazil

²Centre de Mathématiques et de leurs Applications,
Ecole Normale Supérieure de Cachan,
94235 Cachan, France

³Laboratoire de Physique de la Matière Condensée,
Ecole Polytechnique,
91128 Palaiseau, France

(Dated: August 22, 2018)

A surprising similarity is found between the distribution of hydrodynamic stress on the wall of an irregular channel and the distribution of flux from a purely Laplacian field on the same geometry. This finding is a direct outcome from numerical simulations of the Navier-Stokes equations for flow at low Reynolds numbers in two-dimensional channels with rough walls presenting either deterministic or random self-similar geometries. For high Reynolds numbers, when inertial effects become relevant, the distribution of wall stresses on deterministic and random fractal rough channels becomes substantially dependent on the microscopic details of the walls geometry. In addition, we find that, while the permeability of the random channel follows the usual decrease with Reynolds, our results indicate an unexpected permeability increase for the deterministic case, i.e., “the rougher the better”. We show that this complex behavior is closely related with the presence and relative intensity of recirculation zones in the reentrant regions of the rough channel.

PACS numbers: PACS numbers: 05.45.Df, 41.20.Cv, 47.53.+n

Partial differential equations are basic in the mathematical formulation of physical problems. The Laplace equation, for example, is known for its relevance in many fields, namely electrostatics, heat transport, heterogeneous catalysis, and electrochemistry. Although rather simple in form, the Laplace equation can have highly non-trivial solutions, specially if the boundary of the system represents the surface of an irregular object. The role of this particular complexity has been a theme of constant research interest with recent important developments [1, 2, 3]. Much more complex, however, are the Navier-Stokes equations for the description of hydrodynamic flow in irregular geometries. The aim of the present work is first to reveal a surprising analogy between the properties of the solutions of 2d Laplace and Navier-Stokes equations when flow at low Reynolds and proper boundary conditions are imposed on the *same geometry*. In a second step, we present results obtained at higher Reynolds numbers and for distinct types of surface geometry.

The situations we compare and find to be quantitatively similar are displayed in Fig. 1. Figure 1a pictures the simplest Laplacian problem, namely that of a capacitor with a pre-fractal electrode. The complex feature here is the distribution of charge on the irregular electrode or, in mathematical terms, the distribution of the harmonic measure. The recent research on this field has been mainly dedicated to the application of Laplacian transport towards and across irregular interfaces [1, 4, 5]. The system depicted in Fig. 1b corresponds to Stokes flow in a symmetric rough channel with the same geometry as in Fig. 1a. The hydrodynamic quantity which is found to be distributed similarly to the harmonic measure in

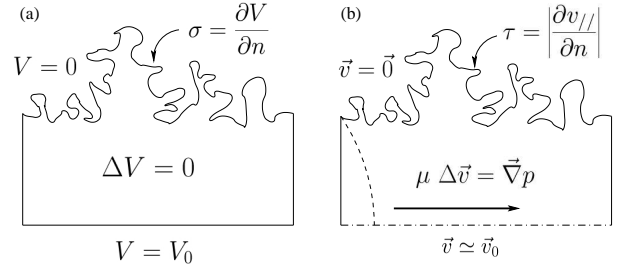


FIG. 1: The two different problems with similar solutions. In (a) we show a capacitor with an irregular electrode. The local charge is obtained from the numerical solution of the Laplace equation with Dirichlet boundary conditions. In (b) we see the analogous problem of flow at low Reynolds number. The stress parallel to the wall channel can be calculated from the solution of the continuity and Stokes ($Re = 0$) equations.

Fig. 1a is the viscous stress along the channel boundary.

To obtain the potential field for the problem in Fig. 1a, one must compute the solution of Laplace equation with a potential $V = 1$ on the counter electrode and zero potential on the irregular electrode (Dirichlet boundary condition). From that, it is then possible to calculate the charge σ_L^i on each elementary unit i of the wall and its corresponding normalized counterpart, $\phi_L^i \equiv \sigma_L^i / \sum \sigma_L^j$. As previously shown [6], the distribution of ϕ_L along the irregular electrode is strongly nonuniform as a consequence of screening effects, being in fact characterized as multifractal. This is a typical situation where the deep regions of the irregular surface support only a very small fraction of the total charge, as opposed to the more ex-

posed parts.

The hydrodynamic question posed here has been triggered by the idea that the design of flowing systems should include the influence of the surface geometry as a possibility for optimal performance. For this, we investigate the flow in a duct of length L and width h whose delimiting walls are identical pre-fractal interfaces with the geometry of a square Koch curve (SKC) [6]. The mathematical description for the fluid mechanics in this channel is based on the assumptions that we have a continuum, Newtonian and incompressible fluid flowing under steady state conditions. The relevant physical properties of the fluid are the density ρ and the viscosity μ . In our simulations, we consider non-slip boundary conditions at the entire solid-fluid interface. In addition, gradientless boundary conditions are assumed at the exit $x = L$, whereas a parabolic velocity profile is imposed at the inlet of the channel. The numerical solution for the velocity and pressure fields in the rough channel is obtained through discretization by means of the control volume finite-difference technique [7]. For our complex geometry, this problem is solved using a structured mesh based on quadrangular grid elements. For example, in the case of the channel with walls that are fourth-generation SKC curves, a mesh of approximately a million elements adapted to the geometry of the interface generates satisfactory results when compared with numerical meshes of higher resolution.

The Reynolds number is defined here as $Re \equiv \rho V h / \mu$, where V is the average velocity at the inlet. In Fig. 2a we show the velocity vector field at low Re located at the self-similar reentrant zones that constitutes the roughness of the irregular channel. Indeed, as depicted in Fig. 2b, by rescaling the magnitude of the velocity vectors at the details of the roughness wall, we can observe fluid layers in the form of consecutive eddies. Although much less intense than the mainstream flow, these recirculating structures are located deeper in the system, and therefore experience closer the landscape of the solid-fluid interface. More precisely, viscous momentum is transmitted laterally from the mainstream flow and across successive laminae of fluid to induce vortices inside the fractal cavity. These vortices will then generate other vortices of smaller sizes whose intensities fall off in geometric progression [8, 9].

Once the velocity and pressure fields are obtained for the flow in the rough channel, we can compute the normalized stress ϕ_S^i at each elementary unit i of the wall, $\phi_S^i \equiv \tau_S^i / \sum \tau_S^j$, where the sum is over the total number L_p of perimeter elements, the magnitude of the local stress is given by $\tau_S = |\partial v_{\parallel} / \partial n|$, the derivative is calculated at the wall element, v_{\parallel} is the local component of the velocity that is parallel to the wall element, and n is the local normal coordinate. The semi-log plot in Fig. 3a shows that the spatial distribution of normalized stresses at the interface is highly heterogeneous, with numerical values in a range that covers more than five orders of magnitude. Also shown in Fig. 3a is the variation along

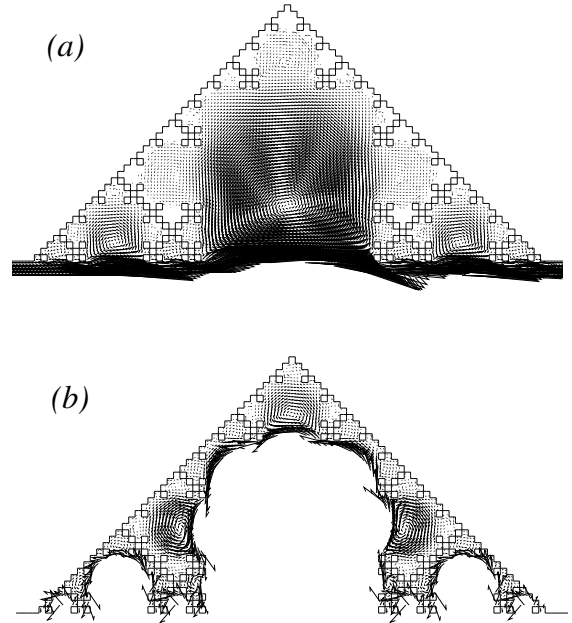


FIG. 2: (a) Vortices in the reentrant zones of the upper half of the (symmetric) pre-fractal roughness channel. The fluid flows steadily from left to right at a low Reynolds number, $Re = 0.01$. (b) Sequence of the smaller eddies at the details of the roughness wall shown in (a). These structures can only be viewed by rescaling the magnitude of the velocity vectors because their intensities fall off in geometric progression.

the interface of the normalized Laplacian fluxes ϕ_L crossing the wall elements of a Laplacian cell with Dirichlet boundary conditions. The astonishing similarity between these two distributions clearly suggests that the screening effect in flow could be reminiscent of the behavior of purely Laplacian systems. As shown in Fig. 3b, this analogy is numerically confirmed through the very strong correlation between local stresses and Laplacian fluxes. These measures follow an approximately linear relationship, namely $\phi_S \propto \phi_L$.

A further analogy can be drawn from the discussion of the notion of *active zone*, as the zone which supports the majority of the charge or current (for the Laplacian field) as well as the shear stress here [1]. For two-dimensional systems subjected to Dirichlet's boundary condition, a fundamental step towards the understanding of the purely Laplacian problem is the mathematical theorem given by Makarov [2]. This theorem states that *the information dimension of the harmonic measure on a singly connected interface of arbitrary geometry in $D = 2$ is exactly equal to 1*. In practical terms, it essentially says that, whatever the shape (perimeter) of an interface, the size of the region where most of the activity takes place is of the order of the overall size L of the system. Here

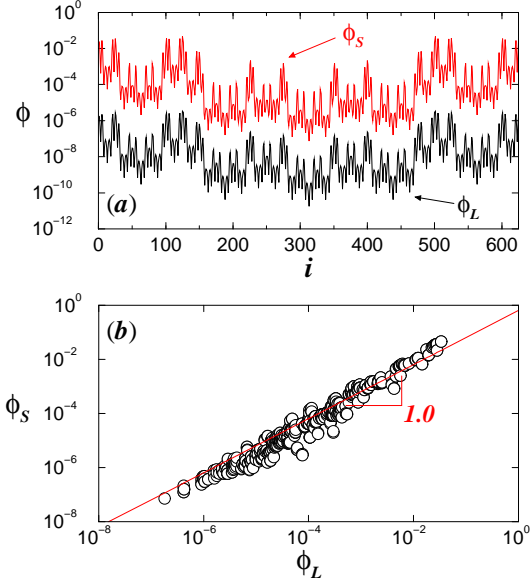


FIG. 3: (a) The (dark) black line is the curvilinear distribution of the logarithm of the normalized shear stresses ϕ_s on the interface along one of the two (symmetric) square Koch curves corresponding to the channel walls. The (light) red line gives the distribution of the logarithm of the normalized Laplacian charges ϕ_L for the analogous electrostatic problem. For better visualization, the distribution of ϕ_L has been shifted downwards. (b) Double-logarithmic plot of ϕ_s versus ϕ_L , with the red line indicating their linear relationship.

we define an *active length* L_a as,

$$L_a \equiv 1 / \sum_{i=1}^{L_p} (\phi_s^i)^2 \quad (1 \leq L_a \leq L_p) . \quad (1)$$

If L_a is equal to the wall perimeter L_p , the entire wall works uniformly. The theorem of Makarov indicates that, on the opposite, for a purely Laplacian field, $L_a \approx L$. The active length therefore provides an useful index to quantify the interplay between the flow and the complex geometry of the interface at the local scale. The results in Fig. 4a (open circles) show that the value of L_a for the square Koch curve remains approximately constant at $L_a/L = 0.55$ for low and moderate Reynolds numbers. This value is consistent with our screening analogy because it indicates that the hydrodynamic stress is mainly concentrated in a subset of the wall whose size is of the order of the system size L . Only at higher Re values, when inertial forces become comparable to viscous forces, one can observe a small increase in L_a . The stress becomes slightly less localized due to the higher relative intensities of the vortices inside the deeper reentrant zones, when compared with the intensities of the correspondent flow structures at low Reynolds conditions.

The usual approach to describe single-phase fluid flow in irregular media (e.g., porous materials and fractures) is to characterize the system in terms of a macroscopic index, namely the permeability K , which relates the av-

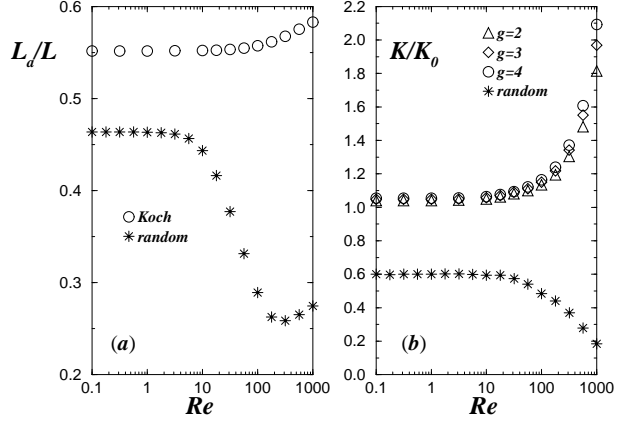


FIG. 4: (a) Semi-log plot showing the dependence of the active length L_a on the Reynolds number Re for the square Koch channel (empty circles) and random Koch channel (stars). In (b) we show the semi-log plot of the variation of the normalized permeability with Re for the random Koch curve (stars) and the second (triangles), third (diamonds) and fourth (circles) generations of the square Koch channel. One observes that the higher is the generation of the pre-fractal SKC, the larger is its permeability.

erage fluid velocity V with the pressure drop ΔP measured across the system, $V = -K \Delta P / \mu L$. Figure 4b (open circles) shows that the permeability of the rough channel for low and moderate Re remains essentially constant at a value that is slightly above but very close to the reference permeability of a two-dimensional smooth channel, namely ($K/K_0 \simeq 1$), with $K_0 \equiv h^2/12$ [10]. Above a transition point at about $Re \simeq 10$, the change in permeability reflects the onset of convective effects in the flow, and therefore the sensitivity of the system to these inertial nonlinearities. Surprisingly, one observes that, instead of decreasing with Re (i.e., a behavior that is typical of disordered porous media), the permeability of the SKC substantially increases. Moreover, as shown in Fig. 4b, the higher the generation of the SKC, the higher is the permeability of the channel for a fixed value of Re above the transition. In other words, “the rougher the better”. These results show that the screening effect of the hierarchical SKC geometry on the flow can be understood in terms of a reduction in the effective non-slip solid-fluid interface. In other words, we can imagine that each vortex present in a given generation of the SKC is in fact replacing one or a set of highly dissipative (non-slip) wall elements of previous SKC of lower generations.

Next we study the fluid flow through a rough channel whose walls are composed of 10 successive and distinct realizations of the random Koch curve (RKC) of third generation. As in the previous case with the deterministic SKC walls, this task is performed here through finite-differences [7], but now with an unstructured mesh of triangular grid elements based on a Delaunay network. Interestingly, the results shown in Fig. 4a (full circles) indicate that the active length L_a of the wall stress cal-

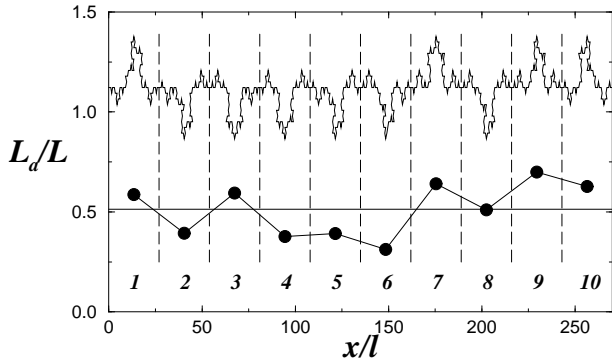


FIG. 5: The active length L_a for each of the 10 wall subsets composing the entire geometry of the random Koch curve channel shown at the top. The dashed lines indicate the boundaries between consecutive subsets, as numbered below. The fluid flows from left to right at $Re = 0.1$.

culated for the entire irregular interface geometry at low values of Re , $L_a/L \simeq 0.46$, is not substantially different from the SKC case, where $L_a/L = 0.55$. In Fig. 5 we show that the ratio L_a/L calculated individually for each of the 10 wall subsets composing the rough channel does not vary significantly from one unit to another. This is a rather unexpected behavior, specially if we consider the complexity of the different geometries involved (see Fig. 5). A similar effect has been observed for the purely Laplacian problem in a random geometry [5]. These facts strongly reinforce our conjecture that the rationale behind the screening effect in flow through rough channels should be based on a general conceptualization that is quite similar to the well established theory for Laplacian systems [2].

As depicted in Fig. 4a, by increasing the Reynolds number, the departure from Stokes flow due to convection at $Re \simeq 10$ results initially in the decrease of L_a/L (calculated over the entire surface) down to a minimum of approximately 0.25 at $Re \simeq 200$. This behavior indicates the presence of long-range flow correlations imposed by inertia among successive wall subsets. More specifically, due to the randomness of these interface units, we can observe either “inward” (e.g., the wall subsets 2, 3, 4, 5, 6 and 8 in Fig. 4) or “outward” protuberances (e.g., the wall subsets 1, 7, 9 and 10 in Fig. 4) composing

the roughness of the channel. Due to the symmetry of the system, the inward elements generate bottlenecks for flow. At high values of Re , the effect of inertia is to induce *flow separation lines* between the mainstream flow at the center of the channel and the flow near the wall, that can be as large as the largest distance between two consecutive bottlenecks. These exceedingly large “stagnation regions” are responsible for the initial decrease in the active length. If we increase even more the Reynolds number, the relative intensities of the vortices in these regions starts to increase. As in the case of the SKC channel, L_a/L starts to increase due to a more distribution of shear stress near the wall.

Finally, in Fig. 4b we show the variation with Re of the permeability for the RKC channel (full circles). In this case, we also observe a transition from linear (constant K) to nonlinear behavior that is typical of experiments with flow through real porous media and fractures [11]. Contrary to the results obtained for the SKC channel, however, the value of K calculated for low Re values is significantly different and smaller than the reference value K_0 of the corresponding smooth channel ($K/K_0 \simeq 0.6$). Once more, this is a consequence of the presence of several bottlenecks in the channel, which drastically reduce the effective space for flow. At high Reynolds, this difference is amplified due to inertial effects.

In summary, we have investigated the effect of deterministic as well as random roughness of 2D channels on local as well as macroscopic flow properties. Our main results are threefold. First, at low Reynolds numbers there exists a very close analogy between the spatial distribution of the local stress on the rough walls and the distribution of charge resulting from the solutions of the Laplace equation for the electric potential in the same geometry. Second, for a fractal deterministic roughness, a surprising increase of the permeability with Reynolds is observed. Moreover, this effect is augmented by increasing the fractal generation of the channel wall so that, paradoxically, “the rougher the better”. Such results could find practical applications in microfluidics and help, for example, to understand the enhanced hydrodynamical features underlying shark-skin effects.

We thank the Brazilian agencies CNPq, CAPES, FUNCAP and FINEP for financial support.

[1] B. Sapoval, Phys. Rev. Lett. **73**, 3314 (1994); B. Sapoval *et al.*, Chem. Eng. Sci. **56**, 5011 (2001).

[2] N. G. Makarov, Proc. London Math. Soc. **51**, 369 (1985); P. Jones and T. Wolff, Acta Math. **161**, 131 (1988).

[3] P. Meakin, H. E. Stanley, A. Coniglio and T. A. Witten, Phys. Rev. A **32**, 2364 (1985); J. H. Kaufman, G. M. Dimino and P. Meakin, Physica A **157**, 656 (1989).

[4] J. S. Andrade Jr. *et al.*, Europhys. Lett. **55**, 573 (2001); Phys. Rev. E **68**, 041608 (2003); Physica A **339**, 296 (2004).

[5] M. Filoche and B. Sapoval, Phys. Rev. Lett. **84**, 26 (2000).

[6] C. J. G. Everts and B. B. Mandelbrot, J. Phys. A: Math. Gen. **25** 1781 (1992).

[7] S. V. Patankar, *Numerical Heat Transfer and Fluid Flow* (Hemisphere, Washington DC, 1980); We use the FLUENT fluid dynamics analysis package (FLUENT Inc.) in this study.

- [8] H. K. Moffat, *J. Fluid. Mech.* **18**, 1 (1964).
- [9] G. Leneweit and D. Auerbach, *J. Fluid Mech.* **387**, 129 (1999).
- [10] R. B. Bird, W. E. Stewart and E. N. and Lightfoot, *Transport Phenomena* (John Wiley & Sons, New York, 1960).
- [11] F. A. L. Dullien, *Porous Media - Fluid Transport and Pore Structure* (Academic, New York, 1979).